Development of ceria-supported ruthenium catalysts effective for various synthetic

reactions

Kenji Wada, Saburo Hosokawa, Masashi Inoue

M. Inoue (Corresponding author)

Department of Energy and Hydrocarbon Chemistry, Graduate School of Engineering,

Kyoto University, Katsura, Kyoto 615-8510, Japan

e-mail: inoue@scl.kyoto-u.ac.jp

Abstract

Our recent results on organic transformations such as C–C bond formation via the activation of stable C–C or C–H bonds and aerobic oxidation of alcohols catalyzed by CeO_2-supported ruthenium are reviewed. A simple, recyclable heterogeneous Ru/CeO_2 catalyst showed excellent activity for sequential transfer-allylation/isomerization of homoallyl alcohols with aldehydes to saturated ketones via the C–C bond activation. While homogeneous ruthenium and rhodium complex catalysts require additives and/or pressurized CO, the reaction with Ru/CeO_2 smoothly proceeded in the absence of any additives. The Ru/CeO_2 catalyst also showed excellent activity for the addition of sp^2 C–H bonds of aromatic ketones to vinylsilanes. The Ru/CeO_2 catalyst also realized the chelation-assisted arylation of stable aromatic C–H bonds with aryl chlorides. The activity of the catalyst was greatly improved by the PPh_3-modification under hydrogen atmosphere prior to the reactions. The catalyst acts heterogeneously without a significant leaching of ruthenium species, indicating that the Ru/CeO_2 catalyst has an advantage over homogeneous catalysts from practical and environmental points of view.

The effects of chemical and physical properties of CeO_2 on the activity of CeO_2-supported noble metal catalysts were examined. Porous CeO_2 powders were prepared by the coagulation of solvothermally synthesized colloidal ceria nanoparticles,

and the thus-prepared CeO_2 powders showed an oxygen migration ability far superior to the CeO_2 samples prepared by the usual precipitation method. The ruthenium catalysts supported on the former CeO_2 powders showed a high activity for the aerobic oxidation of benzyl alcohol. The effects of the pore structure of CeO_2 powders on the activity of the Ru/CeO_2 catalysts are also discussed.

1. Introduction

Of the rare earth oxides, ceria is most widely used as catalysts [1–6], polishing materials, gas sensors [7], ultraviolet absorbents [8], oxygen ion conductors in solid oxide fuel cells [9–10], and so on. Characteristic interactions of CeO_2 with supported noble metal species such as stabilization of the highly dispersed state of noble metal species play important roles in catalysis [1,3,4,6]. Such characteristics lead to the improved performance of noble-metal/CeO_2 catalysts for automobile exhaust conversion [11–13] and many other reactions; for example, Rh/CeO_2 for methane partial oxidation [14] and

N_2O decomposition [15], Pt/CeO_2 for CO oxidation [16] and hydrogenation [17], and Pd/CeO_2 for methanol decomposition [18]. Recently, CeO_2-supported gold catalysts were adopted in organic transformations such as homocoupling of phenylboronic acids [19] and hydrosilylation of aldehydes, ketones, alkenes, imines, and alkynes [20].

Among CeO_2-supported catalysts, the ruthenium catalyst has attracted much attention because of the formation of characteristic surface ruthenium species such as highly-dispersed pentacoordinated ruthenium oxo species [21]. Remarkable activities of the Ru/CeO_2 catalysts have been reported for liquid-phase oxidation of alcohols or aldehydes [22–24], wet oxidation of organic pollutants in waste water [25,26], ammonia synthesis [27], N_2O decomposition [21], complete oxidation of ethyl acetate and propylene [28,29], and other reactions. Recently, $Ce_{1-x}Ru_xO_{2-\delta}$ solid solution was reported as a new oxygen storage material [30]. To further improve the catalytic activity of Ru/CeO_2, systematic investigations on control of their pore structures and surface properties are indispensable. In addition, the application of solid catalysts such as Ru/CeO_2 to various organic transformations as recyclable heterogeneous catalysts is highly desired from practical and environmental points of view.

In this account, we first describe our recent achievements of the Ru/CeO_2-catalyzed C–C bond formations via the selective activation of stable C–C and

C–H bonds. These reactions have significantly broadened the range of organic reactions for which the environmentally benign solid catalysts are applicable. In the latter section, we focus on the contribution of the oxygen migration ability of the CeO_2 support on the catalytic activity of Ru/CeO_2. In addition, systematic control of the pore structure of the Ru/CeO_2 catalysts and the CeO_2 supports is described.

2. Ru/CeO₂-catalyzed organic transformations via stable C–H or C–C bond activation

Homogeneous ruthenium complex catalysts have been extensively investigated because they provide powerful tools in modern organic synthesis [31]. In particular, the asymmetric hydrogenation developed by Noyori *et al*. [32] and the alkene metathesis developed by Grubbs *et al*. [33] are the most prominent achievements realized by ruthenium complex catalysts. In addition, carbon–carbon bond formations via the activation of stable C–H bonds [34,35] and unstrained C–C bonds [36,37] have been achieved by the use of low-valent ruthenium complex catalysts. Despite the excellent activities and selectivities, these homogeneous catalysts have significant drawbacks for practical uses such as the high cost of catalyst production, high sensitivity towards air

and moisture, problems in the catalyst separation, and so on. The use of heterogeneous catalysts is an effective way to overcome these disadvantages. Among the heterogeneous catalysts, oxide-supported catalysts are particularly advantageous because of their low production costs and high thermal and/or chemical stabilities. In most cases, solid catalysts are readily removed from the reaction mixture by simple filtration without leaching of metallic species and can be recycled [38,39]. Therefore, we focused our efforts on the quest for solid oxide-supported ruthenium catalysts that show activities superior to those of homogeneous catalysts for the carbon–carbon bond formation via C–H or C–C bond activation.

Our first target is the transfer-allylation from tertiary homoallylic alcohols to aldehydes via selective cleavage of non-strained carbon–carbon bonds. The reaction of this type was first developed by Kondo *et al*. and several ruthenium–phosphine complexes were found to be effective [40]. Afterwards, Oshima and coworkers reported rhodium complex-catalyzed reactions [41]. For both of the catalysts, however, phosphorous additives, inorganic bases, an excess amount of allylic alcohols, and/or pressurized carbon monoxide are required.

After our extensive survey of oxide-supported catalysts, we found that CeO_2-supported ruthenium catalyst shows an excellent activity for this reaction [42]. As

shown in Table 1, the reaction of homoallylic alcohol (**1a**) with benzaldehyde (**2a**) at 170 ^{o}C in the presence of a catalytic amount of Ru(2.0 wt%)/CeO$_2$, which was prepared by the usual impregnation method by using a THF solution of Ru$_3$(CO)$_{12}$, gave the desired product **4a** in 69% yield together with acetophenone (**3**). Ruthenium catalysts supported on SiO$_2$, Al$_2$O$_3$, TiO$_2$, or MgO did not show any activity at all, indicating that the combination of ruthenium and CeO$_2$ is essential for the generation of catalytically active species. The reaction in the presence of acidic TiO$_2$ or Ru/TiO$_2$ did not give **4a** but gave an indene derivative (**5a**) via intramolecular Friedel-Crafts reaction of **1a**, suggesting that the present transfer-allylation does not proceed via the carbonyl-ene-type pathway catalyzed by Lewis acids [43]. The Ru/CeO$_2$ catalyst was recyclable at least three times without a loss in the activity after calcination at 400 ^{o}C for 30 min, and the ICP-AES analysis revealed that leaching of the ruthenium species from the solid catalysts during the reaction shown in entry 2 of Table 1 was 0.0014 mmol.

(Table 1)

(structure of **5a**)

The reaction of **1a** with a variety of aromatic aldehydes smoothly proceeded to give the desired ketones in moderate to high yields (Table 2). In the reaction for 2 h or less, the major product was a homoallylic alcohol, **6a** (Ar = Ph). This indicates that the present reaction proceeds via transfer-allylation to form intermediates (**6**), followed by the isomerization of **6** to ketones, **4**.

(Table 2)

(Structure of **6**)

The initial step of these reactions might consist of the oxidative addition of an OH group of **1** to an active ruthenium species and the β-allyl elimination to give **3** and an (allyl)ruthenium intermediate, which would react with an aldehyde to give the homoallyl alcohol (**6**). Based on the spectroscopic study of the catalysts, low-valent ruthenium species on the surface of CeO_2 generated *in situ* were considered to be catalytically active. In the XPS study, the Ru $3d_{5/2}$ binding energy in the used catalyst was found to be lower than that in the fresh catalyst, indicating that ruthenium(IV) species was reduced during the reaction.

These results provide the first example of allyl transfer reactions via the

selective cleavage of an unstrained carbon–carbon bond promoted by solid ruthenium catalysts. Note that no additives such as phosphines, amines, or CO were required and the catalyst was recyclable.

Following the success of our first attempt, we speculated that Ru/CeO_2 has the potential to be a good alternative to homogeneous ruthenium complex catalysts. Therefore, we examined the catalytic activity of Ru/CeO_2 towards the addition of aromatic C–H bonds to vinylsilanes [44]. This reaction is one of the most important organic transformations catalyzed by the homogeneous ruthenium complexes [34] and there has been no previous report on the reactions facilitated by solid catalysts. The reaction of α-tetralone (**7a**) with triethoxyvinylsilane (**8a**) in the presence of Ru/CeO_2 and PPh_3 (0.10 mmol, 4 equivalents to Ru species) at 170 ^{o}C for 24 h afforded the desired product **9a** in 99% yield with complete regioselectivity (Table 3). Among the phosphorous additives examined, only PPh_3 and $P(p\text{-F-}C_6H_4)_3$ were effective, and in the absence of these phosphines, the reaction did not proceed. ZrO_2-supported ruthenium catalyst showed an activity comparable to that of Ru/CeO_2, whereas SiO_2-, Al_2O_3-, TiO_2-, or MgO-supported ruthenium catalysts did not show any activity even in the presence of PPh_3.

(Table 3)

Various aromatic ketones bearing either electron donating or withdrawing substituents were applicable as well as heteroaromatic ketones, and the desired alkylated products were produced in the yields of 67 to 96% (at 170 ^{o}C for 24 h) in a completely regioselective manner (Table 4). On the other hand, the scope of alkenes was limited. At present, only **8a** and dimethylethoxyvinylsilane (**8b**) have been found to be applicable, and the reaction of **7a** with other alkenes resulted in very low yields of the desired adducts. Hot filtration of the solid catalyst during the reaction almost completely suppressed further progress of the reaction, indicating that the reaction requires the presence of the solid catalyst, and the leaching of ruthenium species from the catalyst to the reaction mixture was 0.00075 mmol (entry 3 in Table 3). From a practical point of view, it is highly desired that the reaction could be conducted on a large scale without a solvent. The reaction of 35 mmol of **7a** with 80 mmol of **8a** afforded **9a** with a high TON of 837, which is slightly lower than the highest value (1125) reported for homogeneous ruthenium catalysts [35].

(Table 4)

We deduced that a high reaction temperature, 170 ^{o}C, would be required for *in situ* generation of catalytically active species, presumably reduced surface ruthenium phosphine complexes. Therefore, the effects of reductive pretreatment in the presence of phosphines were examined. The treatment of Ru/CeO$_2$ at 100 ^{o}C for 20 min in the presence of PPh$_3$ under H$_2$ (Scheme 1) gave a PPh$_3$-modified Ru/CeO$_2$ catalyst (*x*PPh$_3$−Ru/CeO$_2$, *x* = molar ratio of PPh$_3$/Ru). The thus-modified catalyst showed an activity surprisingly higher than that of the unmodified catalysts and gave **9a** in 99% yield at a significantly lower temperature, 140 ^{o}C (bath temperature, under vigorous toluene reflux), within 90 min. Note that the catalyst reduced in the absence of PPh$_3$ did not show catalytic activity at all, even for the reactions performed in the presence of PPh$_3$.

(Scheme 1)

As shown above, the addition of stable aromatic C–H bonds to vinylsilanes was achieved by Ru/CeO$_2$ or Ru/ZrO$_2$ catalysts with a small amount of PPh$_3$ for the first time, and the reaction smoothly proceeded even under solvent-free conditions. The

11

reductive pretreatment of the Ru/CeO$_2$ in the presence of PPh$_3$ was found to increase the catalytic activity markedly.

On the other hand, the nitrogen-directed arylation of stable aromatic C–H bonds with aryl halides provides a useful pathway for preparing unsymmetrical biaryls with high atomic efficiency [45–47], and several low-valent ruthenium complex catalysts such as [RuCl$_2$(C$_6$H$_6$)]$_2$ with PPh$_3$ [45] or [RuCl$_2$(p-cymene)]$_2$ together with a special kind of phosphorous ligands [46] were reported to be effective for this reaction. However, no previous examples of oxide-supported catalysts effective for reactions of this type have been reported so far.

Recently, we found that Ru/CeO$_2$ or Ru/ZrO$_2$ catalysts are quite effective for the chelation-assisted direct arylation of aromatic C–H bonds [48]. In the absence of phosphorous additives, the Ru/CeO$_2$-catalyzed reaction of benzo[h]quinoline (**10a**) with chlorobenzene (**11a**) at 170 ^{o}C for 18 h regioselectively afforded an arylated product (**12a**) in 89% yield (eq. 1). Again, ruthenium catalysts supported on oxides other than CeO$_2$ or ZrO$_2$ did not show any activities. The reaction with methyl-, fluoro-, and trifluoromethyl-substituted chlorobenzenes gave biaryls in moderate to high yields, while chloroarenes with coordinating substituents such as 1-chloro-4-methoxybenzene (**11g**) could not be used (Table 5). In the presence of a catalytic amount of PPh$_3$, the

reaction of **10a** with **11g** efficiently proceeded, and the addition of PPh$_3$ significantly broadened the scope of the substrates. However, relatively high reaction temperature was still essential.

(eq. 1)

(Table 5)

Therefore, the effects of PPh$_3$-modification of Ru/CeO$_2$ were examined (Table 6). 3PPh$_3$–Ru/CeO$_2$ showed enhanced activity, and the reaction of **10a** with chlorobenzene (**11a**) completed within 6 h at 140 ^{o}C while the reaction with bromobenzene (**11h**) completed within 2 h at 120 ^{o}C. Again, the catalyst reduced in the absence of PPh$_3$ did not show catalytic activity at all, even for the reactions performed in the presence of PPh$_3$. A variety of chloroarenes were applicable for the reaction catalyzed by PPh$_3$-modified Ru/CeO$_2$. The PPh$_3$-modification of Ru/CeO$_2$ catalyst further broadened the scope of applicable haloarenes. In addition to **10a**, other directed C–H activation substrates could be applied (Table 7).

(Table 6)

(Table 7)

The PPh$_3$-modified catalysts were recyclable at least three times without a loss

of activity for the reaction of **10a** and **11a** at 140 $^{\circ}$C (Table 6), and leaching of

ruthenium species into the reaction mixture was 0.00065 mmol. Hot filtration of solid

catalysts completely stopped further progress of the reaction. These results indicate that

Ru/CeO$_2$ and Ru/ZrO$_2$ act as environmentally-benign, recyclable heterogeneous

catalysts effective for direct C–H arylation with a wide range of aryl chlorides.

For the three reactions described above, only CeO$_2$- or ZrO$_2$-supported

ruthenium catalysts showed activity. Although the exact reason is not clear yet, Ru/CeO$_2$

and Ru/ZrO$_2$ showed several characteristic features in the spectroscopic study. The

XRD study showed that the crystallites of RuO$_2$ were present on the surface of SiO$_2$-,

Al$_2$O$_3$-, and MgO-supported catalysts. On the other hand, the ruthenium catalysts

supported on CeO$_2$ or ZrO$_2$ did not exhibit the XRD peaks due to ruthenium phases,

indicating ruthenium species are highly dispersed. (XRD patterns are shown in the

supporting information of ref. [48]). In the diffuse reflectance infrared Fourier transform

(DRIFT) spectra of Ru/CeO$_2$, a strong band was recognized at around 975 cm^{-1}, which

is assignable to ruthenium(IV) oxo species [21]. This band disappeared after the

14

reaction and regenerated by the re-calcination [42,44,48]. Although the distinct band

due to ruthenium oxo species was not recognized on Ru/ZrO$_2$ in the present studies, the

formation of reactive ruthenium–oxygen species has been proposed for the

ZrO$_2$-supported ruthenium catalyst [29,49]. On the other hand, there were no signs of

oxo species for ruthenium catalysts supported on the other oxides [42,44,48]. In the

temperature-programmed reduction with hydrogen (H$_2$-TPR), the fresh Ru/CeO$_2$ and

Ru/ZrO$_2$ catalysts showed reduction peaks at below 60 $^\mathrm{o}$C, indicating that surface

ruthenium species on CeO$_2$ and ZrO$_2$ are easily reduced. On the other hand, the

reduction of ruthenium species on the other supports occurred at above 70 $^\mathrm{o}$C [48].

Based on these data, we deduce, at the present stage, that ruthenium(IV) oxo species is a

good precursor of catalytically active species, and these active species would be

generated *in situ* by the reduction at the beginning of catalytic runs or

PPh$_3$-modification prior to the reaction. The Ru/CeO$_2$-catalyzed C-H alkylation and

arylation are considered to proceed via the chelation-assisted regioselective activation of

the aromatic C-H bond, which have been proposed for the reactions catalyzed by

ruthenium complexes [34,35,45–47], since the regioselectivities of the present reactions

are identical to those catalyzed by the ruthenium complexes. Detailed studies on the

structure of ruthenium species supported on CeO$_2$ or ZrO$_2$ as well as the nature of

catalytically active species of PPh$_3$-modified Ru/CeO$_2$ and detailed reaction mechanisms are now in progress.

3.   Aerobic oxidation of benzyl alcohol on Ru/CeO$_2$ prepared from ceria nanoparticles

The Ru/CeO$_2$ catalyst has high activities for various oxidative reactions such as wet oxidation and combustion of organic compounds, as indicated in the introduction section [21–30]. In this chapter, the performances of the Ru/CeO$_2$ catalysts prepared from various CeO$_2$ powders were compared in terms of the activity for aerobic oxidation of benzyl alcohol as a model reaction. Note that Vocanson *et al*. reported that Ru/CeO$_2$ catalyst is effective for the oxidation of various alcohols [22].

Table 8 compares the properties and activities of two representative Ru/CeO$_2$ catalysts [50]. One catalyst, Ru/CeO$_2$-A, was prepared by the addition of a 3M NaOH solution to an aqueous solution (500 mL) containing ceria colloids (in 100 mL of 2-methoxyethanol; CeO$_2$, 3–4 g), RuCl$_3$•nH$_2$O, and formalin (10 mL) until the pH of the solution became 11, followed by calcination at 500 ℃ for 3 h in air. Another catalyst

designated as Ru/CeO$_2$-B was prepared using an aqueous solution (500 mL) containing

Ce(NO$_3$)$_3$•6H$_2$O (0.030 mol) in place of the ceria colloidal solution for the recipe of

Ru/CeO$_2$-A. Furthermore, two pure CeO$_2$ powders were prepared: CeO$_2$-A by the

coagulation of ceria colloidal nanoparticles with a 3 M aqueous NaOH solution

followed by washing and calcination at 400 $^{\circ}$C for 3 h, and CeO$_2$-B by the usual

precipitation method using an aqueous solution of Ce(NO$_3$)$_3$•6H$_2$O and a 3 M NaOH

solution.

As shown in Table 8, Ru/CeO$_2$-A possessed a surface area slightly smaller than

that of Ru/CeO$_2$-B; however, Ru/CeO$_2$-A exhibited higher catalytic activity for the

oxidation of benzyl alcohol, clearly indicating that surface area is not an important

factor governing the activities. The XRD analysis of both the catalysts gave similar

patterns in which only the peaks due to CeO$_2$ were recognized, suggesting that

ruthenium species on both of the catalysts were well-dispersed.

(Table 8)

The H$_2$-TPR profiles of Ru/CeO$_2$- B, a physical mixture of RuO$_2$–α-Al$_2$O$_3$, and

CeO$_2$-B are shown in Figure 1. The TPR profile of CeO$_2$-B showed two reduction peaks,

one at 300–500 ºC and the other at a higher temperature >500 ºC. The former peak has

been assigned to the reduction of the surface Ce^{IV} species, and the latter peak has been

ascribed to the reduction of lattice Ce^{IV} species [11]. On the other hand, ruthenium

species on Ru/CeO_2-B were reduced at a temperature lower than that required for the

reduction of RuO_2, indicating the formation of highly dispersed surface Ru=O species

on Ru/CeO_2-B [21,51]. Note that in the profile of Ru/CeO_2-B, the low-temperature

reduction peak of CeO_2 disappeared, and the amount of H_2 consumed by Ru/CeO_2-B at

<100 ºC was much larger than the theoretical value (0.40 mmol g^{-1}) calculated on the

basis of the following equation assuming that all the ruthenium species are in the form

of RuO_2:

$$RuO_2 + 2H_2 \ \rightarrow \ Ru^0 + 2H_2O$$
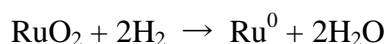
The H_2 consumption by Ru/CeO_2-B (0.72 mmol g^{-1}, Table 8) was almost equal to the

sum of H_2 uptakes of RuO_2–α-alumina (0.27 mmol g^{-1}) and CeO_2-B at the lower

temperature range (0.41 mmol g^{-1}). These results indicate that the ruthenium species

accelerate the reduction of surface Ce^{IV}, probably due to migration of surface oxygen

species from CeO_2 to ruthenium species.

(Figure 1)

Based on the above discussion, the ability of surface oxygen migration of CeO_2 supports is expected to contribute to the oxidation of benzyl alcohol. Therefore, the redox properties of CeO_2-A and -B were compared by the repeated TPR analyses (Figure 2 and Table 9). The sample was subjected to the TPR study up to 500 ℃, then oxidized with O_2 at 300 ℃, and again subjected to the TPR procedure up to 950 ℃. As judged from the low temperature peak areas of 1st and 2nd TPR measurements, 81 % of the original oxidized-surface of CeO_2-A was recovered during the re-oxidation process, while only 61 % was recovered for CeO_2-B. These results clearly indicate that the surface of CeO_2-A, a single component CeO_2 sample prepared by the coagulation of the ceria colloidal nanoparticles, was more easily reduced and re-oxidized than the CeO_2 sample prepared by the precipitation method from $Ce(NO_3)_3$. The higher activity of Ru/CeO_2-A is brought about by the inherent high surface oxygen mobility of the CeO_2 support itself.

(Figure 2)

(Table 9)

19

4. Pore structure control of ceria nanoparticles

Nanoparticles of metal oxides generally show characteristic features and are expected to be excellent supports for highly active catalysts. So far, several preparation methods of ceria nanoparticles have been developed [52–54]. One of the authors reported that the solvothermal reaction of Ce metal in 2-methoxyethanol yielded a transparent colloidal solution containing ceria nanoparticles with a particle size of *ca.* 2 nm [55,56].

In this chapter, the pore-structure control of CeO_2 prepared by coagulation of solvothermally synthesized ceria colloidal nanoparticles is described. High surface energy of colloidal nanoparticles induced a strong tendency to coagulate by the addition of alkaline solutions, and subsequent calcination produced CeO_2 powders with micro- or meso-pores originating from the voids between primary ceria nanoparticles [57]. The pore structure of CeO_2 powders was partly controlled by the selection of alkaline solutions [58]. Table 10 compares crystallite sizes and pore structures of various CeO_2 powders, which were coagulated by the addition of aqueous solutions of various bases (1 M, 200 mL) to ceria colloidal solutions, followed by calcination at 300 $^{\circ}$C for 3 h. Whereas the crystallite sizes of all the CeO_2 powders after the coagulation and calcination were in the range of 4–5 nm, their pore structures were significantly affected

by the coagulants. In particular, the CeO_2 powders prepared by using NaOH and $(NH_4)_2CO_3$ had large surface areas over 120 m^2g^{-1}. The nitrogen adsorption/desorption isotherms of the CeO_2 powders are shown in Figure 3. The CeO_2 powders prepared using Na_2CO_3 and NH_4OH showed typical type-I isotherms characteristic of microporous materials. The powders prepared using NaOH and NH_4HCO_3 showed E-type hysteresis loops based on the de Boer classification, which were responsible for ink-bottle or tubular pores formed between primary particles. For the powders coagulated with $(NH_4)_2CO_3$ and $NaHCO_3$, large amounts of nitrogen were adsorbed at the high P/P_0 range over 0.8, indicating the formation of macropores. The XRD and TG analyses of powders coagulated with $(NH_4)_2CO_3$ and $NaHCO_3$ before calcination indicate the presence of a small amount of crystalline $Ce_2(CO_3)_3 \cdot 8H_2O$ formed from atmospheric CO_2 and cerium ions remaining in the solution after the solvothermal reaction. Evolution of CO_2 gas from $Ce_2(CO_3) \cdot 8H_2O$ during calcination is one reason for the formation of macropores.

(Table 10)

(Figure 3)

The effects of the pore-structure of CeO_2 powders on the catalytic activity of Ru/CeO_2 for the liquid-phase aerobic oxidation of benzyl alcohol were examined [58] and Table 11 shows the results. The Ru/CeO_2 catalysts were prepared as follows; the prescribed amount of $RuCl_3 \cdot nH_2O$ was dissolved in a suspension of CeO_2 powders in water. After the addition of 5 mL of a 37% aqueous formaldehyde solution, the suspension was heated at 80 ^{o}C for 0.5 h and then a 3 M NaOH solution was added until the pH of the suspension became ca. 11. The precipitate was dried at 80 ^{o}C and calcined at 500 ^{o}C for 3 h. The catalysts prepared using the CeO_2 powders with relatively large meso- and macro-pore surface area exhibited higher activities to give benzaldehyde in the yields of about 58% (entries 4–6). No other products were detected in GC analysis. A control experiment showed ca. 10% benzaldehyde was adsorbed on the catalyst.

The XRD patterns of poorly active Ru/CeO_2 catalysts prepared using NaOH, NH_4OH, and Na_2CO_3 showed peaks due to RuO_2 crystallites. The H_2-TPR study also indicates marked effects of coagulants on the state of surface ruthenium species of Ru/CeO_2. The highly active catalysts showed a sharp peak at ~75 ^{o}C due to ruthenium(IV) oxo species [21,51]. On the other hand, the poorly active catalysts showed two peaks at 75 ^{o}C and 90 ^{o}C; the latter peak is due to crystalline RuO_2. These results indicate that the Ru/CeO_2 catalysts prepared using CeO_2 powders with large

surface areas in meso- and macro-pore regions generally possess highly dispersed surface ruthenium(IV) oxo species and showed excellent catalytic activities.

(Table 11)

The pore structure of CeO_2 powders derived from colloidal nanoparticles can also be controlled by the concentration of the NaOH coagulant [59]. High concentration of the NaOH solution gave the CeO_2 coagulate having well-developed mesopores, while BET surface areas were not affected by NaOH concentration. The 10 M NaOH solution partially dissolved ceria nanoparticles because of their high surface energy. It is known that ceria dissolves in acidic solutions in the presence of hydrogen peroxide, and hardly dissolves in alkaline solutions [60]. Actually, the pore structure of the CeO_2 sample prepared by a conventional precipitation method using a $Ce(NO_3)_3$ solution is not affected by the concentration of the NaOH solution. Therefore, characteristic pore structure caused by the coagulation of ceria colloidal particles with a highly concentrated NaOH solution was thought to be due to the nature of the ceria colloidal nanoparticles. As expected, the Ru/CeO_2 catalyst prepared by coagulation of the ceria nanoparticles with the 10 M NaOH solution showed higher activity and higher yield

(73%) than the catalyst prepared using 1M NaOH (65%).

(Table 12)

(Figure 4)

5.   Concluding remarks

We have demonstrated the excellent activities of the Ru/CeO_2 catalysts for the

transfer-allylation from tertiary homoallylic alcohols to aldehydes [42], the addition of

aromatic C–H bonds to vinylsilanes [44], and the direct arylation of aromatic C–H

bonds by chloroarenes [48]. These reactions had only been achieved by the use of

homogeneous transition-metal complex catalysts so far, and therefore, the works in this

account provided the first successful examples of solid-catalysts that achieved

carbon–carbon bond formation via the activation of non-strained C–C bonds or

non-activated stable C–H bonds. These results indicate the wide possibility of Ru/CeO_2

as an attractive, environmentally benign alternative to homogeneous ruthenium

complex catalysts.

In addition, we showed that CeO_2 powders of high surface areas can be

prepared by the coagulation of ceria colloidal nanoparticles with suitable coagulants followed by calcination. The mobility of surface oxygen of the CeO_2 support as well as the dispersion state of ruthenium species are found to be key factors for the oxidation activity of Ru/CeO_2 [50]. Furtheremore, the pore structures of the thus-obtained CeO_2 powders are controlled by the selection of the coagulant, and the ruthenium catalyst supported on CeO_2 possessing meso- and/or macro-pores shows high activity for the oxidation of benzyl alcohol [58,59].

For further development of Ru/CeO_2 catalysts having excellent activities for a greater diversity of the reactions, precise control of the surface ruthenium species, migration ability of surface oxygen, and pore structure would be required. Detailed investigation on the control of the properties of CeO_2 shown in the latter parts clearly indicates the possibility for further development of the CeO_2-based catalysis, for example, more effective Ru/CeO_2 catalysts for a wide range of organic transformations including C–C and/or C–H bond activation.

Technology, Japan.

References

1. Trovarelli A, Catalysis by ceria and related materials, in: Hutchings GJ (Ed.), Catalytic Science Series, Imperial College Press., London, 2002.

2. Le Normand F, Hilaire L, Kili K, Krill G, Maire G (1988) J Phys Chem 92:2561.

3. Kašpar J, Fornasiero P, Graziani M (1999) Catal Today 50:285.

4. Bera P, Patil KC, Jayaram V, Subbanna GN, Hegde MS (2000) J Catal 196:293.

5. Bedrane S, Descorme C, Duprez D (2002) Catal Today 75:401.

6. Boaro M, Vicario M, de Leitenburg C, Dolcetti G, Trovarelli A (2003) Catal Today 77:407.

7. Lee JH (2003) J Mater Sci 38:4247.

8. Li R, Yabe S, Yamashita M, Momose S, Yoshida S, Yin S, Sato T (2002) Solid State Ionics 151:235.

9. Steele BCH (1999) Nature 400:619;

10. Steele BCH, Heinzel A (2001) Nature 414:345.

11. Yao HC, Yao YFY (1984) J Catal 86:254.

12. Gandhi HS, Graham GW, McCabe RW (2003) J Catal 216:433.

13. Christou SY, Costa CN, Efstathiou AM (2004) Top Catal 30:325.

14. Seo HJ, Yu EY (2005) J Ind Eng Chem 11:681.

15. Imamura S, Tadani J, Saito Y, Okamoto Y, Jindai H, Kaito C (2000) Appl Catal A 201:121.

16. Bera P, Gayen A, Hegde MS, Lalla NP, Spadaro L, Frusteri F, Arena F (2003) J Phys Chem B 107:6122.

17. Imamura S, Higashihara T, Saito Y, Aritani H, Kanai H, Matsumura Y, Tsuda N (1999) Catal Today 50:369.

18. Imamura S, Denpo K, Kanai H, Yamane H, Saito Y, Utani K, Matsumura Y (2001) J Jpn Petrol Inst 44:293.

19. Carrettin S, Guzman J, Corma A (2005) Angew Chem Int Ed 44:2242.

20. Corma A, González-Arellano C, Iglesias M, Sánchez F (2007) Angew Chem Int Ed 46:7820.

21. Hosokawa S, Nogawa S, Taniguchi M, Utani K, Kanai H, Imamura S (2005) Appl Catal A Gen 288:67.

22. Vocanson F, Guo YP, Namy JL, Kagan HB (1998) Synth Comm 28:2577.

23. Ji H, Mizugaki T, Ebitani K, Kaneda K (2002) Tetrahedron Lett 43:7179.

24. Ebitani K, Ji H, Mizugaki T, Kaneda K (2004) J Mol Catal A 212:161.

25. Barbier J Jr., Delanoë F, Jabouille F, Duprez D, Blanchard G, Isnard P (1998) J Catal 177:378.

26. Imamura S, Fukuda I, Ishida S (1988) Ind Eng Chem Res 27:718.

27. Izumi Y, Iwata Y, Aika K (1996) J Phys Chem 100:9421.

28. Mitsui T, Matsui T, Kikuchi R, Eguchi K (2009) Top Catal 52:464

29. Hosokawa S, Fujinami Y, Kanai H (2005) J Mol Catal A Chemical 240:49.

30. Singh P, Hegde MS (2009) Chem Mater 21:3337.

31. Murahashi S (Eds.) (2004) Ruthenium in Organic Synthesis, Wiley-VCH, Weinheim.

32. Noyori R (2003) Adv Syn Catal 345:15.

33. Grubbs RH (2004) Tetrahedron 60:7117.

34. Murai S, Kakiuchi F, Sekine S, Tanaka Y, Kamatani A, Sonoda M, Chatani N (1993) Nature 366:529.

35. Martinez R, Simon MO, Chevalier R, Pautigny C, Genet JP, Darses S, J Am Chem Soc (2009) 131:7887.

36. Kondo T, Mitsudo T (2005) Chem Lett 34:1462.

37. Mitsudo T, Suzuki T, Zhang SW, Imai D, Fujita K, Manabe T, Shiotsuki M, Watanabe Y, Wada K, Kondo T (1999) J Am Chem Soc 121:1839.

38. Sheldon RA, Downing RS (1999) Appl Catal A Gen 189:163.

39. Kaneda K (2007) Synlett 999.

40. Kondo T, Kodoi K, Nishinaga E, Okada T, Morisaki Y, Watanabe Y, Mitsudo T (1998) J Am Chem Soc 120:5587.

41. Hayashi S, Hirano K, Yorimitsu H, Oshima K (2006) J Am Chem Soc 128:2210.

42. Miura H, Wada K, Hosokawa S, Sai M, Kondo T, Inoue M (2009) Chem Commun 4112.

43. Lee CLK, Lee CHA, Tan KT, Loh TP (2004) Org Lett 6:1281 and references therein.

44. Miura H, Wada K, Hosokawa S, Inoue M (2010) ChemCatChem accepted.

45. Oi S, Fukita, S, Hirata N, Watanuki N, Miyano S, Inoue Y (2001) Org Lett 3:2579.

46. Ackermann L (2005) Org Lett 7:3123.

47. Özdemir I, Demir S, Çetinkaya B, Gourlaouen C, Maseras F, Bruneau C, Dixneuf PH (2008) J Am Chem Soc 130:1156.

48. Miura H, Wada K, Hosokawa S, Inoue M (2010) Chem Eur J 16:4186.

49. Guglielminotti E, Boccuzzi F, Manzoli M, Pinna F, Scarpa M (2000) J Catal 192:149.

50. Hosokawa S, Hayashi Y, Imamura S, Wada K, Inoue M (2009) Catal Lett 129:394.

51. Hosokawa S, Kanai H, Utani K, Taniguchi Y, Saito Y, Imamura S (2003) Appl Catal B Environ 45:181.

52. Yamamoto S, Kakihana M, Kato S (2000) J Alloys Compd 297:81.

53. Masui T, Fujiwara K, Machida K, Adachi G, Sakata T, Mori H (1997) Chem Mater 9:2197.

54. Hirano M, Kato E (1996) J Am Ceram Soc 79:777.

55. Inoue M, Kimura M, Inui T (1999) Chem Commun 975.

56. Kobayashi T, Hosokawa S, Iwamoto S, Inoue M (2006) J Am Ceram Soc 89:1205.

57. Kobayashi T, Iwamoto S, Inoue M (2006) J Alloys Compd 408–412:1149.

58. Hayashi Y, Hosokawa S, Imamura S, Inoue M (2007) J Ceram Soc Jpn 115:592.

59. Hayashi Y, Hosokawa S, Inoue M (2010) Microporous Mesoporous Mater 128:115.

60. Cotton FA, Wilkinson G (1966) Advanced Inorganic Chemistry: A Comprehensive Text, second ed., John Wiley & Sons, New York, pp. 1067–1068.

Captions for Figures and Schemes

Scheme 1 Effect of PPh$_3$-modification of Ru/CeO$_2$ catalyst in H$_2$ towards addition of a C-H bond of α-tetralone to to triethoxyvinylsilane [44]

Figure 1 TPR profiles of Ru/CeO_2-B, RuO_2–α-Al_2O_3 (RuO_2 was physically mixed with α-Al_2O_3), and CeO_2- B [50]. Heating rate 5 ^{o}C min^{-1}, catalyst loading 0.10 g, 2.0% of H_2 in Ar (30 mL min^{-1}). Expanded profiles in the temperature range of 50–150 ^{o}C are shown in b).

Figure 2 Repeated TPR profiles (lower) and the temperature diagram for the experiment (upper) [50].

Figure 3 Nitrogen adsorption/desorption isotherms of the selected CeO_2 powders coagulated with aqueous solutions (1 M) of (a) $NaHCO_3$, (b) NaOH, (c) Na_2CO_3, (d) $(NH_4)_2CO_3$, (e) NH_4HCO_3, and (f) NH_4OH, calcined at 300 ^{o}C [58].

Figure 4 Nitrogen adsorption/desorption isotherms of the selected CeO_2 powders coagulated with (a) 1 M, (b) 5 M, and (c) 10 M aqueous NaOH solutions, followed by calcination at 300 ^{o}C [59].

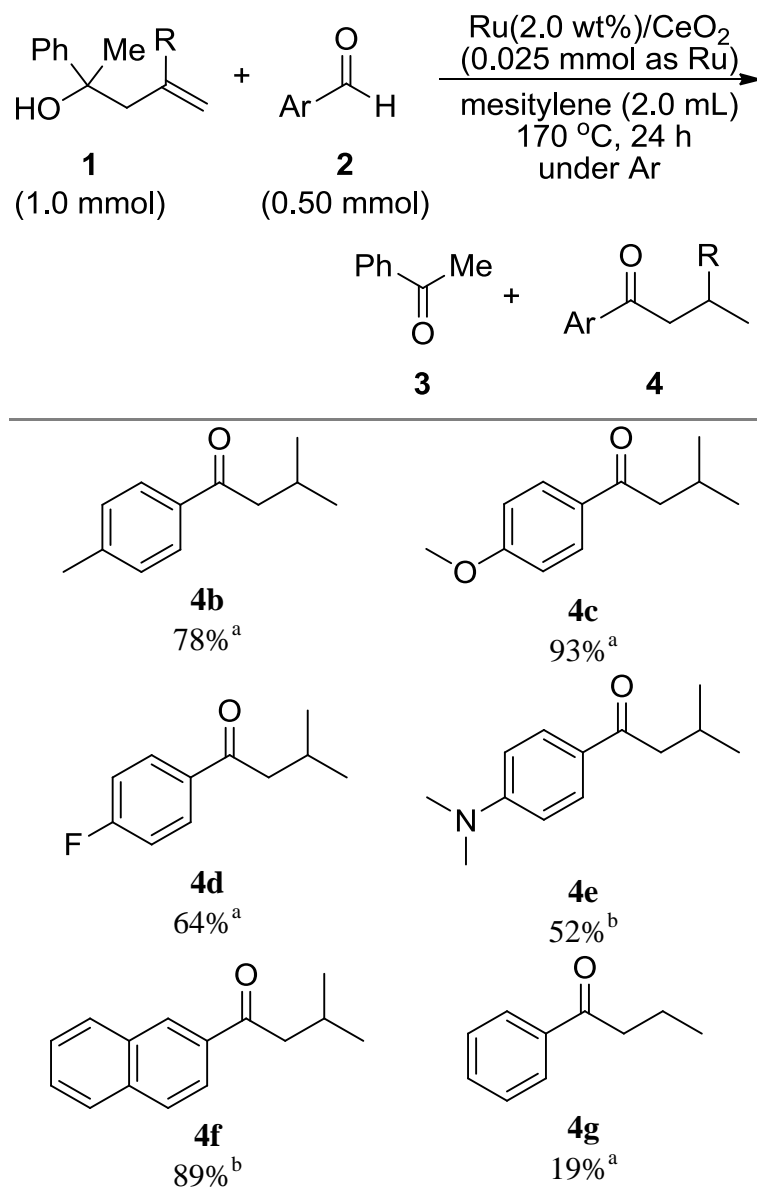**Table 1** Effect of ruthenium catalysts for allyl transfer reaction [42]

Ph Me
|
HO
1a
(1.0 mmol)

+

O
‖
Ph   H
2a
(0.50 mmol)

Ru(2.0 wt%)/support
(0.025 mmol as Ru)
→
mesitylene (2.0 mL)
170 °C, 24 h
under Ar

Ph   Me

O
3

+

O
‖
Ph
4a
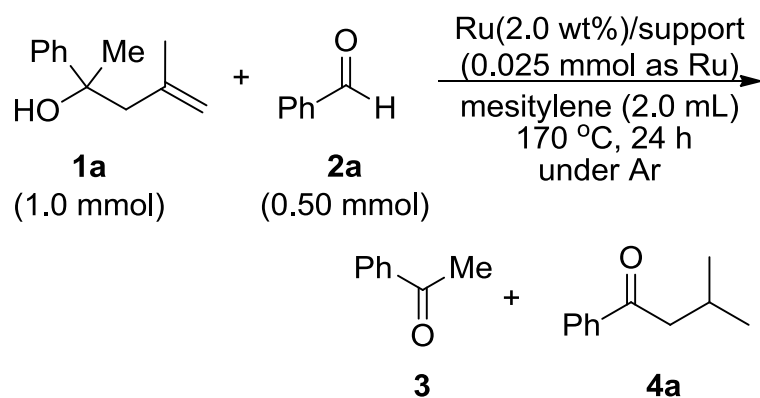
Entry	Catalyst	Yield [%][a,b]
1	CeO_2	0
2	Ru/ CeO_2	69
3	Ru/ SiO_2	0
4	Ru/ Al_2O_3	0
5	Ru/ TiO_2	0[c]
6	Ru/ MgO	0
7	$Ru_3(CO)_{12}$	15

[a] Determined by GLC.
[b] Yield based on **2a**.
[c] Acidic TiO_2 and Ru/TiO_2 catalysts gave **5a** via intramolecular Friedel-Crafts reaction of **1a**.

Table 2 Scope of substrates for Ru/CeO$_2$-catalyzed allyl transfer reaction [42]

4b	4c
78%[a]	93%[a]

4d	4e
64%[a]	52%[b]

4f	4g
89%[b]	19%[a]

[a] Determined by GLC.
[b] Isolated yields.

Table 3 Effect of ruthenium catalysts for addition of a C-H bond of α-tetralone to triethoxyvinylsilane [44]
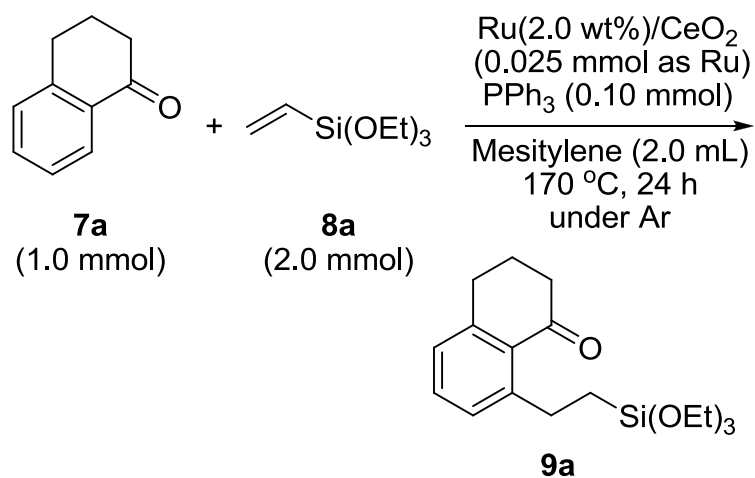
Entry	Catalyst	Yield [%]^{a,b}
1	Ru/CeO$_2$	0^{c,d}
2	Ru/CeO$_2$	78^c
3	Ru/CeO$_2$	99
4	Ru/ZrO$_2$	99
5	Ru/SiO$_2$	0
6	Ru/Al$_2$O$_3$	0
7	Ru/TiO$_2$	0
8	Ru/MgO	0
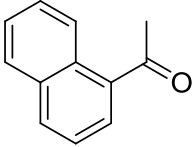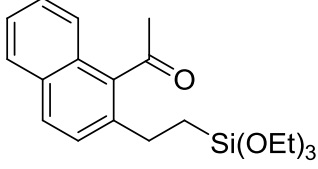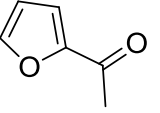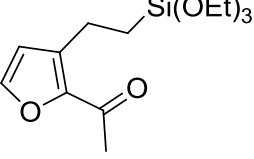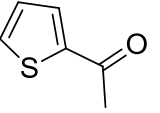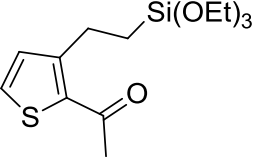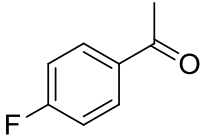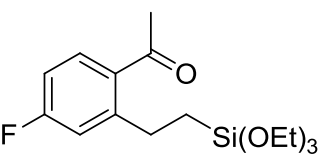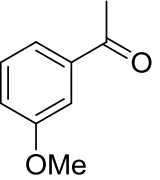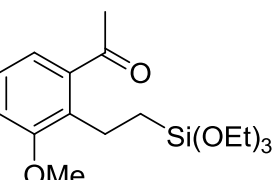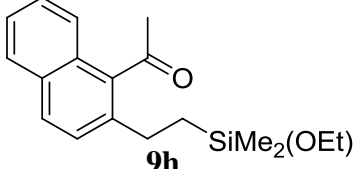
[a] Determined by GLC.
[b] Yield based on **7a**.
[c] Reaction time 6 h.
[d] Without PPh$_3$.

Table 4 Scope of substrates for Ru/CeO$_2$-catalyzed addition of C-H bonds of aromatic ketones to vinylsilanes[a] [44]

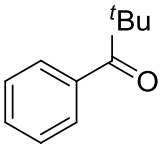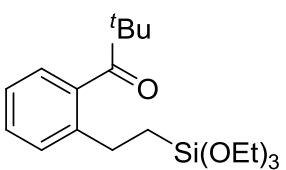| Entry	**7**	**8**	Product	Yield [%][b]
1	**7b**	**8a**	**9b**	96
2	**7c**	**8a**	**9c**	67
3	**7d**	**8a**	**9d**	94
4	**7e**	**8a**	**9e**	91 (53:47)[c]
5	**7f**	**8a**	**9f**	90 (100:0)[c]
6	**7g**	**8a**	**9g**	84 (100:0)[c]
7	**7b**	**8b**	**9h**	84

[a] Reaction conditions: **7**, 1.0 mmol; **8**, 2.0 mmol; Ru/CeO$_2$, 0.025 mmol as Ru atom; mesitylene, 2.0 mL; 170 °C; 24 h.

[b] Isolated yields.

[c] The percentages of mono- and di-substituted products are given in parentheses.

36

Table 5 Scope of substrates for Ru/ZrO$_2$-catalyzed direct arylation of benzo[h]quinoline with aryl chlorides [48]

10a (1.0 mmol)   **11** (1.5 mmol)

Ru(2.0 wt%)/ZrO$_2$
(prepared from [RuCl$_2$(CO)$_3$]$_2$)
(0.050 mmol as Ru)
KF (2.0 mmol)
NMP (2.0 mL), 170 °C
24 h, under Ar

12

11a 94%[a]	**11b** 72%
11c 60%	**11d** 62%
11e 69%	**11f** 92%
11g 0%	**11g** 70%[b]
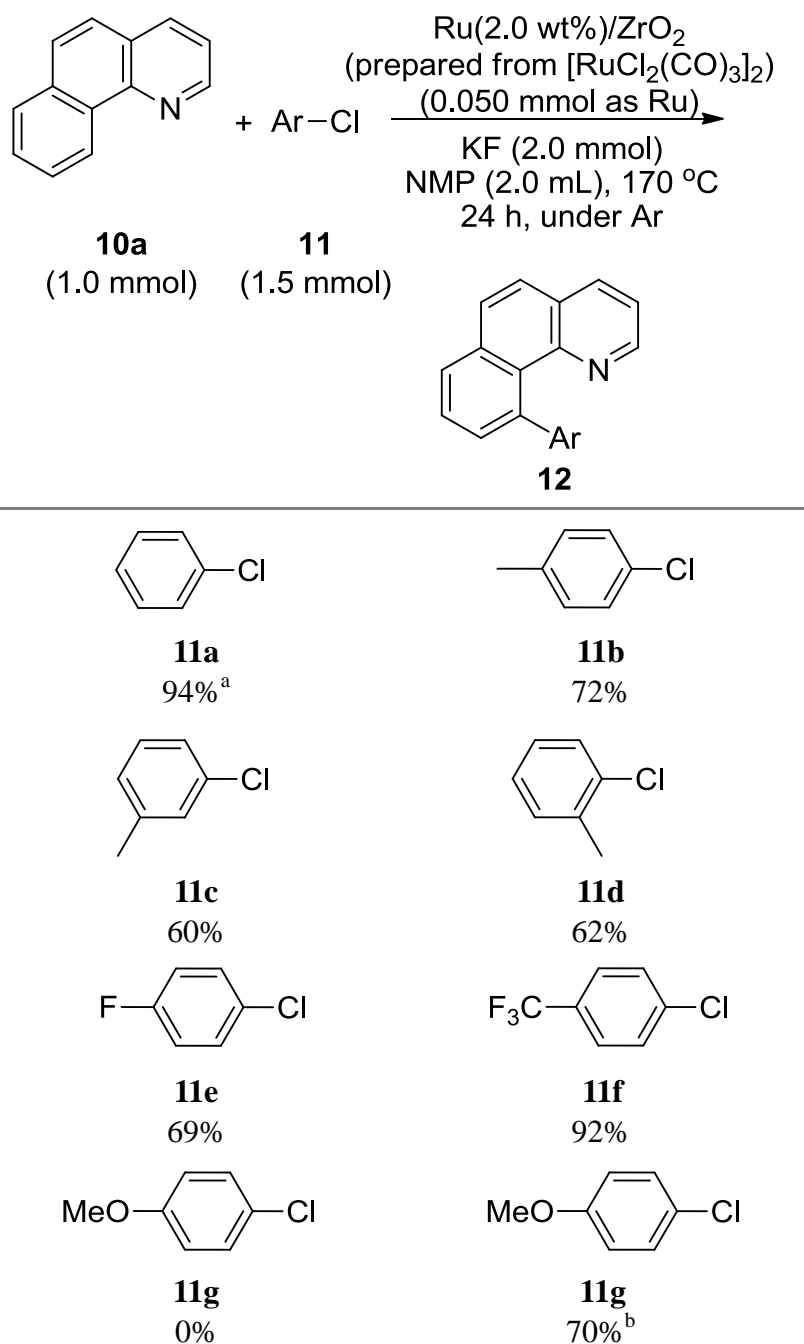
[a] Reaction for 18 h.
[b] With 0.10 mmol of PPh$_3$.

Table 6 Scope of substrates for PPh$_3$-modified Ru/CeO$_2$-catalyzed direct arylation of benzo[*h*]quinoline with aryl halides [48]

10a
(0.50 mmol)

11
(0.75 mmol)

3PPh$_3$-Ru(2.0 wt%)/CeO$_2$
(prepared from [RuCl$_2$(CO)$_3$]$_2$)
(0.025 mmol as Ru)
K$_2$CO$_3$ (1.0 mmol)
NMP (2.0 mL), 140 ^{o}C
under Ar

12

11a
94% (6 h)

11b
96% (6 h)

11f
86% (12 h)

11g
96% (12 h)

11h
96% (120 ^{o}C, 2 h)

11i
95% (3 h)

11j
91% (5 h)

11k
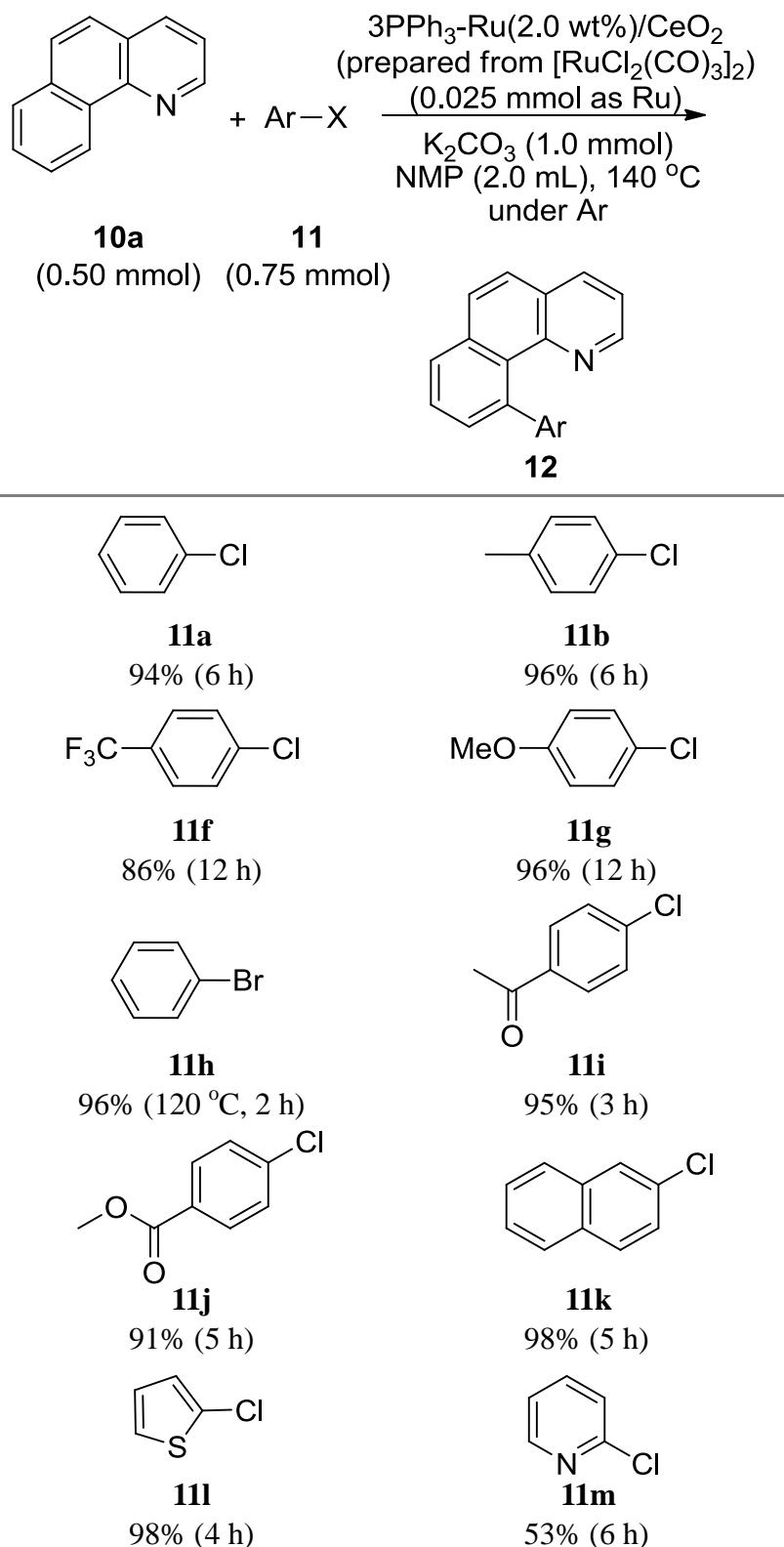98% (5 h)

11l
98% (4 h)

11m
53% (6 h)

Table 7 Scope of substrates for PPh$_3$-modified Ru/CeO$_2$-catalyzed direct arylation with 4-chloroacetophenone [48]

3PPh$_3$-Ru(2.0 wt%)/CeO$_2$
(prepared from
[RuCl$_2$(CO)$_3$]$_2$)
(0.025 mmol as Ru)

K$_2$CO$_3$ (1.0 mmol)
NMP (2.0 mL), 140 ^{o}C
under Ar

10
(0.50 mmol)

11i
(0.75 mmol)

12

13

10b 94% (3 h)
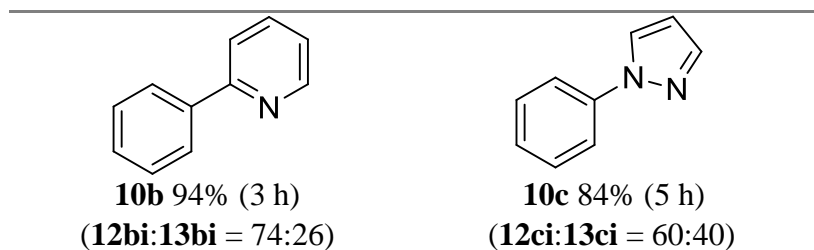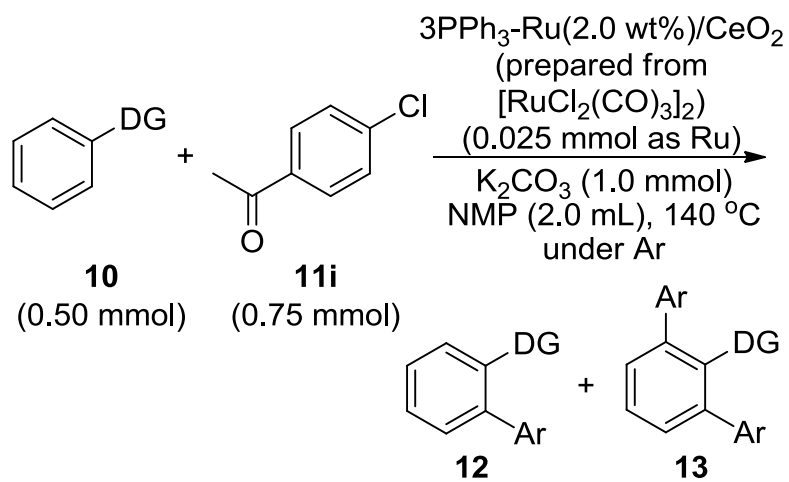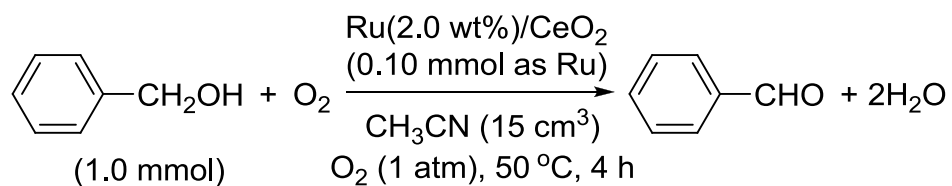(**12bi**:**13bi** = 74:26)

10c 84% (5 h)
(**12ci**:**13ci** = 60:40)

Table 8 Preparation, properties and catalytic activity of Ru(2.0 wt %)/CeO$_2$ toward the liquid-phase oxidation of benzyl alcohol [50]

$$\text{C}_6\text{H}_5\text{—CH}_2\text{OH} + \text{O}_2 \xrightarrow[\begin{array}{c}\text{CH}_3\text{CN (15 cm}^3\text{)}\\\text{O}_2\text{ (1 atm), 50 }^\circ\text{C, 4 h}\end{array}]{\begin{array}{c}\text{Ru(2.0 wt\%)/CeO}_2\\\text{(0.10 mmol as Ru)}\end{array}} \text{C}_6\text{H}_5\text{—CHO} + 2\text{H}_2\text{O}$$

(1.0 mmol)

Entry	Catalyst	Ce source	BET surface area [m^{2}g^{-1}]	H$_2$ consumption [mmol g^{-1}][a]	Benzaldehyde yield [%]
1	Ru/CeO$_2$-A	ceria colloidal nanoparticles	135	0.87	60
2	Ru/CeO$_2$-B	Ce(NO$_3$)$_3$•6H$_2$O	142	0.72	36

[a] Estimated by TPR experiment.

Table 9 Redox properties of CeO_2 powders prepared by different methods followed by calcination at 400 ^{o}C [50]

Entry	CeO_2	Ce source	BET surface area $[m^2g^{-1}]$	H_2 consumption $[mmol \, g^{-1}]$	
				1st run	2nd run
1	CeO_2-A	ceria colloidal nanoparticles	103	0.36 (L)[a]	0.29 (L)[a] (81%)[b] 0.54 (H)[c]
2	CeO_2-B	$Ce(NO_3)_3 \cdot 6H_2O$	139	0.41 (L)[a]	0.25 (L)[a] (61%)[b] 0.43 (H)[c]

[a] Estimated from the area of low temperature peak (< 500 ^{o}C) of the H_2-TPR study.
[b] Percentage of the area of low temperature peak in the 2nd run versus that of 1st run.
[c] Estimated from the area of high temperature peak (> 500 ^{o}C) of the H_2-TPR study.

Table 10 Characterization of the CeO$_2$ powders coagulated by various bases followed by calcination[a] and Catalytic activity of Ru(2.0 wt %)/CeO$_2$ toward the liquid-phase oxidation of benzyl alcohol at 50 $^{\circ}$C for 4 h [58]

Entry	Coagulant	Crystallite size [nm]	Total surface area [m^{2}g^{-1}][b]	Benzyl alcohol conversion [%][c]	Benzaldehyde yield [%][d]
1	NaOH	5.2	132	42.3	37.1
2	NH$_4$OH	5.2	111	32.5	28.4
3	Na$_2$CO$_3$	4.6	67	16.8	8.6
4	(NH$_4$)$_2$CO$_3$	4.8	152	79.6	58.0
5	NaHCO$_3$	4.2	79	81.2	58.3
6	NH$_4$HCO$_3$	5.2	92	81.4	57.8
7	NaOH[b]	-	-	53.0	35.5

[a] At 300 $^{\circ}$C for 3 h in air.

[b] Estimated by the *V-t* plot.

[c] Determined by GLC.

[d] Prepared by coprecipitation method from Ce(NO$_3$)$_3$•6H$_2$O.

Table 11 Pore structures of the CeO$_2$ powders prepared by coagulation or precipitation with NaOH solutions with various concentrations followed by the calcination[a] [59]

Entry	Precursor	NaOH [M]	Total pore volume [cm^{3}g^{-1}]	BET surface area [m^{2}g^{-1}]	Amount of Ce ions dissolved [ppm (%)[b]]
1	ceria colloidal nanoparticles	1	0.097	122	0.82 (0.008)
2		5	0.135	123	-[c]
3		10	0.184	124	16.00 (0.147)
4	Ce(NO$_3$)$_3$•6H$_2$O	1	0.267	167	0.64 (0.006)
5		5	0.287	167	-[c]
6		10	0.280	166	0.11 (0.001)

[a] Calcined at 300 ^{o}C for 3 h in air.

[b] Percentages of cerium ions dissolved per CeO$_2$ samples (3.5g) during the coagulation.
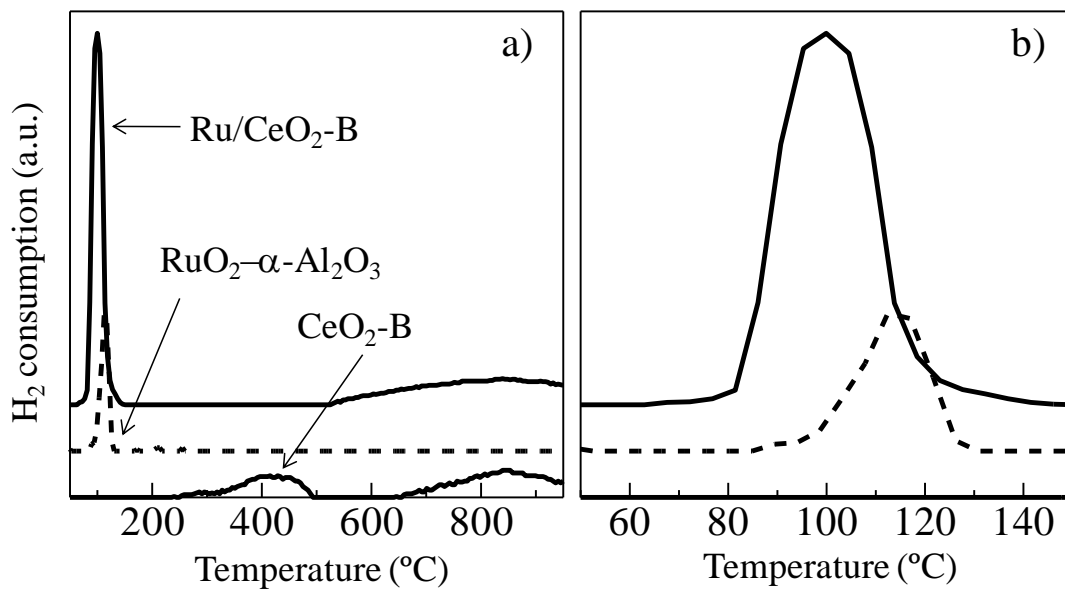
[c] Not measured.

Figure 1 TPR profiles of Ru/CeO$_2$-B, RuO$_2$–α-Al$_2$O$_3$ (RuO$_2$ was physically mixed with α-Al$_2$O$_3$), and CeO$_2$-B [50]. Heating rate 5 $^{\circ}$C min^{-1}, catalyst loading 0.10 g, 2.0% of H$_2$ in Ar (30 mL min^{-1}). Spectra b) enlarged spectra a) from 50 to 150 $^{\circ}$C.
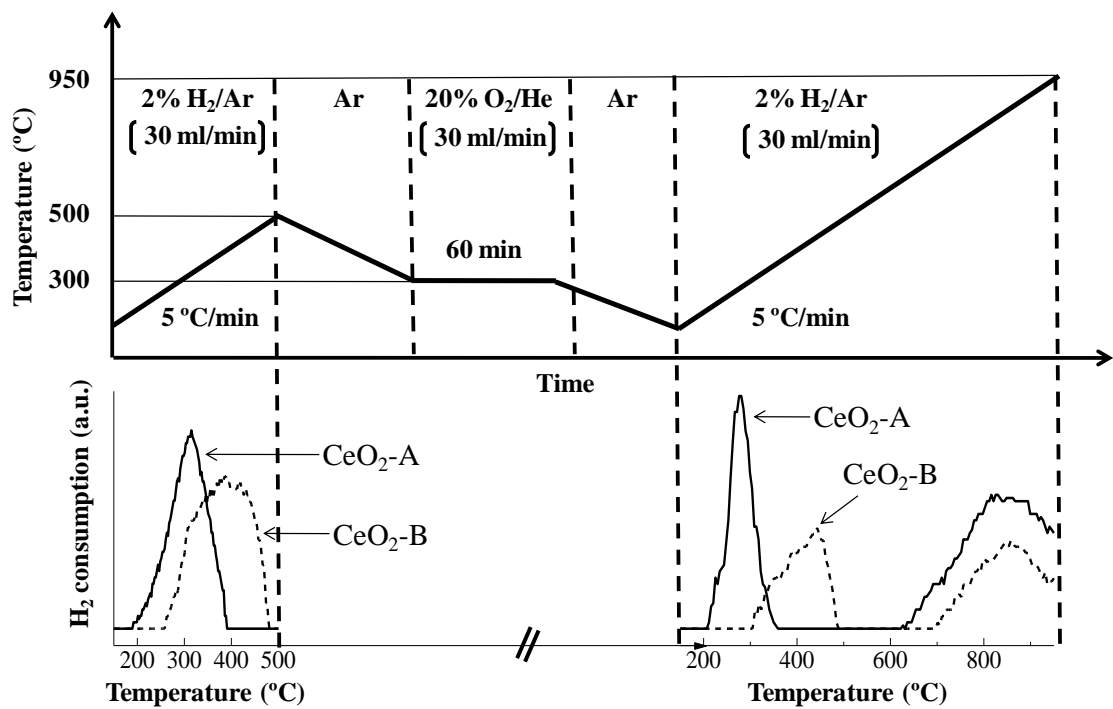
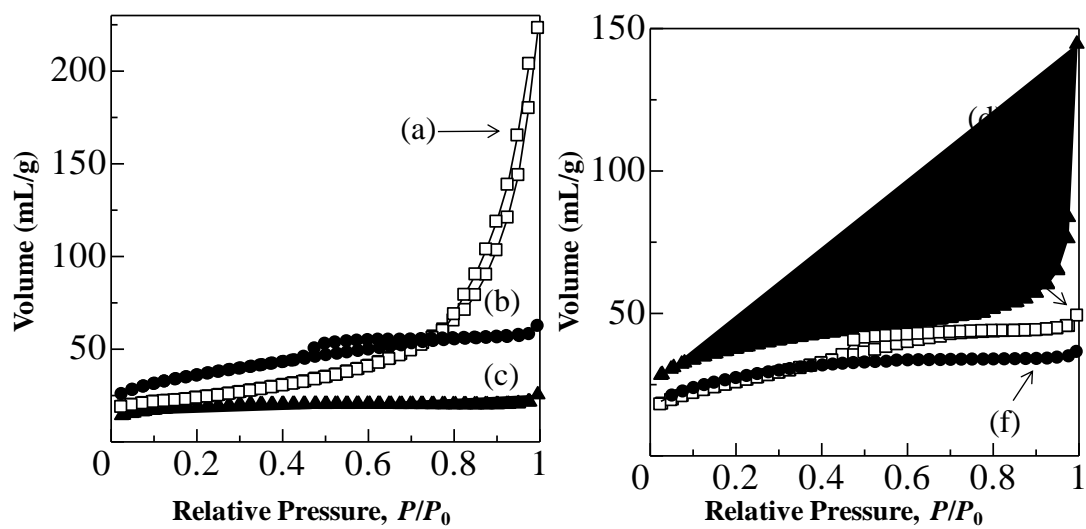**Figure 2** The temperature diagram for the repeated TPR experiments [50].

Figure 3 Nitrogen adsorption/desorption isotherms of the selected CeO_2 powders coagulated with aqueous solutions (1 M) of (a) $NaHCO_3$, (b) NaOH, (c) Na_2CO_3, (d) $(NH_4)_2CO_3$, (e) NH_4HCO_3, and (f) NH_4OH, calcined at 300 ^{o}C [58].
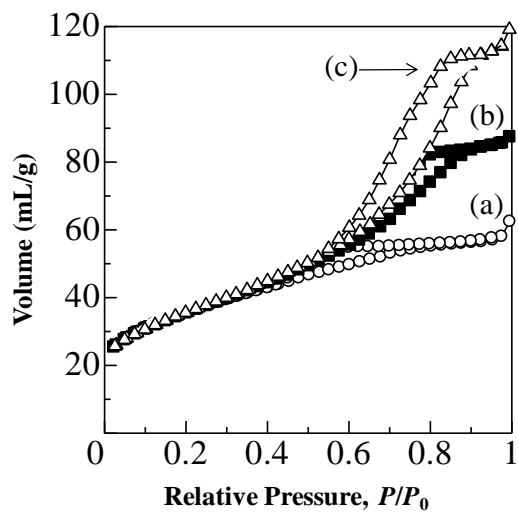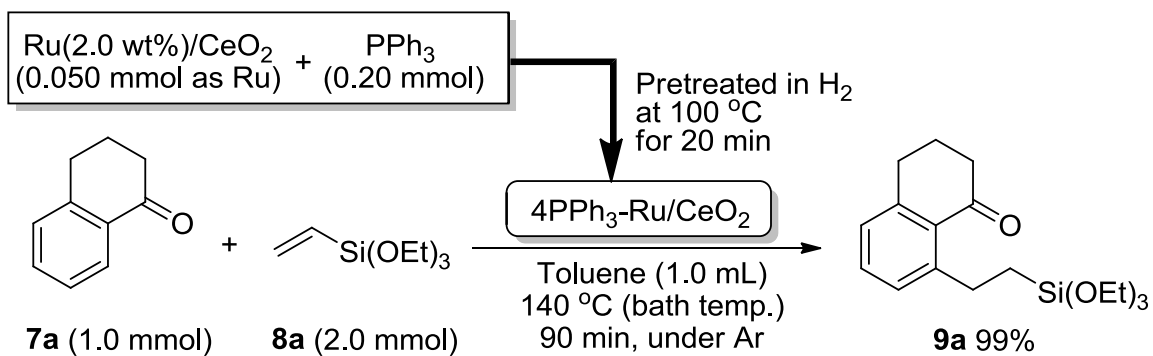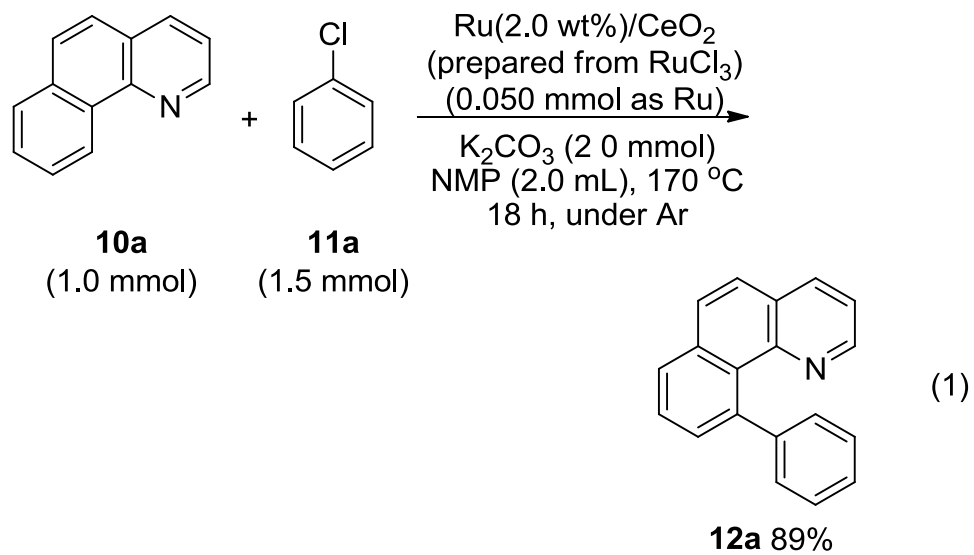
Figure 4 Nitrogen adsorption/desorption isotherms of the selected CeO_2 powders coagulated with (a) 1 M, (b) 5 M, and (c) 10 M aqueous NaOH solutions, followed by the calcination at 300 ^{o}C [59].

Ru(2.0 wt%)/CeO$_2$ (0.050 mmol as Ru) + PPh$_3$ (0.20 mmol)

Pretreated in H$_2$ at 100 ^{o}C for 20 min

4PPh$_3$-Ru/CeO$_2$

Toluene (1.0 mL)
140 ^{o}C (bath temp.)
90 min, under Ar

7a (1.0 mmol)   **8a** (2.0 mmol)   **9a** 99%

(Scheme1)

(Eq. 1)

10a
(1.0 mmol)

+

11a
(1.5 mmol)

Ru(2.0 wt%)/CeO$_2$
(prepared from RuCl$_3$)
(0.050 mmol as Ru)
$\longrightarrow$
K$_2$CO$_3$ (2 0 mmol)
NMP (2.0 mL), 170 ^{o}C
18 h, under Ar

(1)

12a 89%

(Structures of **5a** and **6**)

5a

OH

Ar

6